Construction and Building Materials 270 (2021) 121492

Contents lists available at ScienceDirect

Construction and Building Materials

journal homepage: www.elsevier.com/locate/conbuildmat

Durability of GFRP reinforcing bars in seawater concrete

Carlos N. Morales *, Guillermo Claure, Alvaro Ruiz Emparanza, Antonio Nanni

Department of Civil Architectural and Environmental Engineering, University of Miami, Coral Gables, FL 33146, USA

HIGHLIGHTS

- Physical and mechanical characterizations of aged GFRP bars were performed.
- Accelerated aging exposure has an effect on tensile strength retention.
- SEM images and EDS analysis were used to evaluate microstructural integrity.
- No chemical degradation was detected after environmental conditioning.
- Exponential degradation model is in good agreement with experimental data.

ARTICLE INFO

Article history:
Received 27 August 2020
Received in revised form 19 October 2020
Accepted 24 October 2020
Available online 13 November 2020

Keywords:
Glass FRP
Seawater concrete
Durability
Environmental degradation
Mechanical properties
Microstructures
Marine
Service life

ABSTRACT

This paper presents an experimental study that investigated the durability performance of unstressed glass fiber-reinforced polymer (GFRP) bars embedded in concrete mixed with seawater (seawater concrete). GFRP bars were extracted from concrete elements made with two different seawater concrete mix designs and exposed to different environmental conditions for 1, 6, 12, and 24 months. The concrete samples' exposure environments consisted of typical field conditions of a subtropical region and seawater at 60 °C as an accelerated aging method. The mechanical test results of GFRP bars are reported in residual capacities of tensile strength, longitudinal elastic modulus, transverse shear strength, and apparent horizontal shear strength. Furthermore, the physical evaluations are in terms of glass transition temperature (T_g) and microstructural integrity through scanning electron microscopy (SEM) images and energy-dispersive X-ray spectroscopy (EDS) analysis. Among all tested properties, tensile strength was the most affected by environmental conditioning. Based on an exponential degradation model, the long-term prediction of the tensile strength capacity was on average 92% under typical field exposure and 72% under the more aggressive conditioning (seawater at 60 °C).

1. Introduction

The corrosion of steel reinforcement is one of the main causes of chemical deterioration in reinforced concrete (RC) [1,2]. The replacement of conventional steel bar reinforcement by corrosion-resistant materials has been evaluated over the years [3,4]. Fiber reinforced polymer (FRP) composites bars have been under constant development to be used as internal reinforcement for concrete structure due to its high-strength, lightweight, and, most importantly, non-corrosive properties [5,6]. Among pultruded FRP bars, glass fiber reinforced polymer (GFRP) bars are the most widely used [7]. In addition to the mentioned benefits, the use of this type of non-corrosive material provides an alternative to replace fresh water with seawater in the production of concrete, since the main reason that prohibits the use of seawater in reinforced concrete structures is due to its high presence of chloride that favors the corrosion of steel reinforcement [8,9].

However, it is widely known that the durability of FRP bars can be affected by harsh environmental factors such as high temperatures and moisture content, chemical/alkaline attack from the surrounding medium, and ultraviolet radiation [6]. The degradation mechanisms are mainly related to the type and quality of the constituents (e.g., fiber, sizing, and resin matrix), the manufacturing process, the phenomenon of matrix plasticization, and the integrity of the fiber–matrix interface [10,11].

Since the widespread use of FRP reinforcement for internal concrete structure began in the 1980 s [3] and nearly all reinforced concrete structures have been designed to have a service life of more than 40 years [6], the vast majority of the available data on real-life long-term performance is limited. Gooranorimi and Nanni [12] conducted a study examining GFRP bars made of E-glass fiber

* Corresponding author.
E-mail address: cnm32@miami.edu (C.N. Morales).

https://doi.org/10.1016/j.conbuildmat.2020.121492
0950-0618/

and vinyl ester resin that were retrieved from an overhang portion of a concrete deck of a bridge located in Texas (U.S.) after more than a decade of service. Through micrograph analysis, they concluded that the extracted GFRP bars preserved their microstructural integrity with no visible damage after 15 years of field exposure. Benzecry et al. [13] validated these results by reporting a calculated reduction in tensile stress of 2.13% of GFRP coupons obtained from the same bridge after 17 years in service.

Numerous efforts have been made to assesses and predict the long-term durability performance of FRP reinforcing bars based, primarily, on simulated laboratory testing [6]. Table 1 shows a summary of the physical and residual properties of GFRP bars used in other relevant research studies. For comparison purposes, these studies were selected because they share some similarities with the study presented here, either in terms of the type of constituents (e.g., type of fiber and/or resin), bar diameter, surrounding medium, temperature, or time of exposure. The bars in these other research projects are commercially available GFRP bars typically compliant with standards such as ASTM D7957 [14].

Most of the studies have been carried out using accelerated aging techniques in which bare FRP bars are immersed in detrimental solutions at elevated temperatures to evaluate their physical and mechanical integrity over time [10,15–19]. This approach has been suggested to be more severe than in-service real-life weathering [10,19–21]. For instance, in a durability study conducted by Chen et al. [21] bare and concrete-embedded GFRP bars (E-glass/vinyl ester) exposed to accelerated aging environments were evaluated. In the study, after 2 months of exposure to simulated pore solution at 60 °C, the tensile strength retention of the bare GFRP bars was 52%, while for the GFRP bars that were embedded in concrete the strength retention was 61% after 3 months of exposure. They concluded that the simulated environments were more adverse for bare GFRP bars than for bars embedded in concrete and the test results should be considered as conservative.

Instead of exposing bare bars to aggressive solutions, researchers have also evaluated the behavior of FRP bars embedded in concrete, providing a more realistic behavior of the actual degradation they might experience as internal reinforcement. Fergani et al. [22] investigated the durability and degradation of GFRP bars (ECR-glass/vinyl ester) exposed to different conditioning parameters for up to 9 months. Specifically, 8-mm nominal diameter unstressed GFRP bars embedded in concrete and conditioned in tap water at 60 °C showed tensile strength retention in the range between 80% and 59%. Almusallam et al. [23] investigated the effect of different environmental conditionings exclusively on tensile properties of 12-mm diameter GFRP bars (E-glass/vinyl ester) that were embedded in concrete for 6, 12, and 18 months. The residual tensile strength results revealed that specimens conditioned in tap water at 50 °C showed more degradation than those exposed to seawater at the same temperature. These retentions ranged from 83% and 76% for tap water conditioning, while those exposed to seawater ranged between 86% and 84%.

In another study, Robert et al. [24] conducted accelerated tests to evaluate the durability performance of mortar-wrapped GFRP bars (E-glass/vinyl ester). After 8 months of exposure to tap water at 50 °C, they reported tensile strength retention of the 12-mm diameter GFPR bars embedded in moist concrete of 84%. Furthermore, in a different durability study, Robert et al. [25] evaluated the effect of saline solution (3% NaCl) at different temperatures on the same type of mortar-wrapped GFRP bars. The tensile strength retention after 12 months of exposure to the saline solution at 50 °C was 89% of the initial strength. Finally, in a recent short-term durability study, Jia et al. [26] investigated tensile strength retention of 9.5-mm diameter GFRP bars (E-glass/vinyl ester) embedded in concrete that were exposed to different solutions and ambient humidity. The results showed that after 4 months of conditioning at 60 °C, the specimens subjected to tap water and saline solution experienced strength retention of 61.6% and 60.7%, respectively.

Table 1
Summary of characteristics, strength retention, and conditioning regimes of GFRP bars in previous studies.

Reference	Glass type/resin matrix	Diameter (mm)	Tensile strength retention (%)	Tensile modulus retention (%)	Conditioning	
					(surrounding medium/solution-temperature-duration*)	pH (solution)
[15]	E/VE	9.53	38	–	ALK-60–4	13.6
			59	–	ALK-60–4	12.7
[16,17]	E/Epoxy	6.3	80.1	–	ALK-55–2	13.4
			89.6	132	ALK-55–2	12.7
[18]	E/VE	12.0	75.9	99.1	ALK-50–18	12.5–13
			75.5	97.4	TW-50–18	–
			87.2	97.4	SW-50–18	–
[19]	E/Epoxy	9.2	82.6	103	ASW-60–3	8.1
			67.8	96	ALK-60–3	13.4
[20]	E/VE	9.5	96	95.2	TW-72–2 †	7
			88	92.7	ALK-64–2 †	12.8
[21]	E/VE	9.53	52	–	ALK-60–2	13.6
			61	–	CON/ALK-60–3	12.7
[22]	ECR/VE	8.0	90	99	CON/TW-20–9	–
			59	99	CON/TW-60–9	–
[23]	E/VE	12.0	76	91	CON/TW-50–18	–
			84	94	CON/SW-50–18	–
			78	91	CON/ALK-50–18	12.5–13
[24]	E/VE	12.7	84.4	~97.7	CON/TW-50–8	12.15 ‡
[25]	E/VE	12.7	89.1	~111.8	CON/ASW-50–12	–
[26]	E/VE	9.5	61.6	–	CON/TW-60–4	–
			60.7	–	CON/ASW-60–4	–
[9]	ECR/VE	15.8	79	88	SWCON/SW-60–24	–
[27]	-/Epoxy	8.0	85	–	SWCON/TW-60–15	–
		9.0	50	–	SWCON/TW-60–15	–

Note: *=months; E = E-glass; VE = vinyl ester; ALK = alkaline; TW = tap water; SW = seawater; ASW = artificial seawater; CON = concrete; SWCON = seawater-mixed concrete; †=sustained load 19–29%; ‡=pH of concrete.

Only a few studies have been undertaken to evaluate the long-term durability performance of FRP bars embedded in concrete made with seawater (seawater concrete) instead of fresh water [28]. Hence, El-Hassan et al. [27] examined the strength retention of two types of GFRP bars (8 mm and 9 mm in diameter), made of continuous glass fiber impregnated in epoxy resin, that were embedded in seawater-contaminated concrete. Based on test results, extracted GFRP bars retain between 85% and 50% of their tensile strength after 15 months of exposure to tap water at 50 °C. More recently, Khatibmasjedi et al. [9] conducted a study to examine the effect of seawater-mixed concrete on the long-term properties of GFRP bars. The study consisted of casting seawater concrete elements reinforced with 15.8-mm diameter GFRP bars made of ECR-glass/vinyl ester resin and exposing them to accelerated aging conditioning. They reported that after 24 months of exposure to seawater at 60 °C, the extracted GFRP bars retained 79%, 88%, 75%, and 74% of their initial tensile strength, tensile modulus, transverse shear strength, and horizontal shear strength, respectively.

The purpose of this study is to evaluate residual physico-mechanical properties of unstressed GFRP bars embedded in seawater concrete up to 24 months of exposure. Therefore, different concrete mixes made with seawater and environmental conditioning were assessed. The selected conditionings were chosen to reproduce field conditions and highly aggressive environmental exposure (laboratory accelerated aging). Accordingly, this evaluation provides insight on the long-term durability performance of GFRP bars embedded in seawater concrete, which in turn may allow for a more realistic approach to assess degradation mechanisms and implement design guidelines

2. Experimental program

2.1. Materials

2.1.1. GFRP bar specimens

The pultruded GFRP bars used in this study had a nominal diameter of 9.5 mm (No. 3) and were made of continuous ECR-glass fibers impregnated in a vinyl ester resin. The surface enhancement consisted of a double helically-fiber-wrapped surface creating a small 45° braided surface pattern undulation. The physical and mechanical characterization of pristine (as-received) GFRP bars were determined according to the established tests method indicated in the ASTM D7957 [14]. The property, test method, experimental value, and standard deviation of each test are given in Table 2. For these unconditioned reference values, a minimum of five (5) specimens per test method were tested.

2.1.2. Surrounding concrete

The residual properties of GFRP bars were evaluated using bar segments retrieved from RC slabs that were made with seawater concrete and exposed to different environmental conditions. The GFRP-RC slabs had a span of 1524 mm and were constructed with a cross-sectional area of 152 mm × 304 mm (Fig. 1) and a length of 1828 mm with a clear cover of 19 mm measured from the tension face of the concrete to the surface of the GFRP bar. The environments evaluated in this study were typical field conditions (FC) of a subtropical region of South Florida (U.S.) and seawater (SW) at 60 °C as an accelerated aging method. This latter test protocol was achieved by completely immersing the GFRP-RC slabs into seawater curing tanks at a thermostatically controlled temperature of 60 °C. The average recorded ambient temperature and relative humidity (RH) for the typical field environment were 25 °C and 71.2%, respectively.

Two different seawater concrete mix designs were evaluated. The selected concrete mix designs were based on the Infravation-funded research project named SEACON [30], where an extensive and thorough assessment of the hardened properties of seawater concrete was performed. Both seawater concrete mix designs had a target 28-days compressive strength of 38 MPa. The seawater concrete mix designs proportions go as follows: the mix design denoted as "Type-F" consisted of Portland cement type I/II (332 kg/m^3), fly ash (83 kg/m^3), coarse aggregate (1038 kg/m^3), fine aggregate (612 kg/m^3), and seawater (168 kg/m^3), while the mix design identified as "Type-S" comprised of Portland cement type I/II (208 kg/m^3), slag (208 kg/m^3), coarse aggregate (997 kg/m^3), fine aggregate (691 kg/m^3), and seawater (158 kg/m^3). The seawater used to mix the concrete, as well as for the accelerated aging conditioning, was obtained directly from Biscayne Bay, FL (U.S.) with a pH value of 8.23. Further details on the chemical composition of the seawater used in this study are provided in parallel studies [9,31]. The nomenclature of the tested specimens was based on the mix design (F or S), environmental condition (FC or SW), and temperature (25 °C or 60 °C). For example, "F-FC25" for elements with mix design "Type-F" exposed to field conditioning, "FC", at a temperature of 25 °C.

Concrete cylinders of both mix designs with a diameter of 100 mm and a height of 200 mm were cast and exposed to the same environmental conditioning and time of exposure as the GFRP-RC slabs to evaluate the mechanical and durability performance of concrete. At the end of 24 months, four (4) cylinders

Table 2
Physical and mechanical characterization of the GFRP bars.

	Property	Unit	Test Method	Value	SD
Physical properties	Effective diameter	mm	ASTM D7205	9.56	0.02
	Cross-sectional area	mm^2	ASTM D792	71.81	0.35
	Density	kg/m^3	ASTM D792	2179.6	4.73
	Fiber content	% by weight	ASTM D2584	85.06	0.21
		% by volume	SEM*	71.09	4.46
	Void content	% by volume	SEM*	0.67	0.23
	Glass transition temperature (DMA)	°C	ASTM E1640	112.8	1.70
	Moisture absorption at 24 h	%	ASTM D570	0.055	0.01
	Moisture absorption at saturation	%	ASTM D570	0.127	0.01
Mechanical properties	Tensile strength	MPa	ASTM D7205	822.23	38.7
	Tensile modulus	GPa	ASTM D7205	55.04	1.08
	Ultimate tensile strain	%	ASTM D7205	1.49	0.08
	Transverse shear strength	MPa	ASTM D7617	192.81	6.42
	Horizontal shear strength	MPa	ASTM D4475	44.85	2.41

* Analysis of 11% of the total cross-sectional area of the GFRP bar by digital images processing of SEM micrographs taken equally distributed at the edge, center, and in-between of the GFRP bar [29].

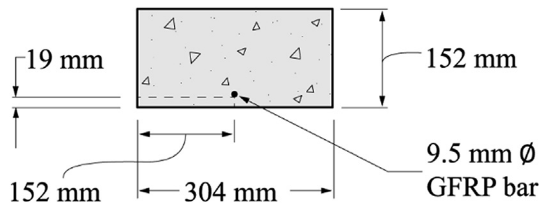

Fig. 1. Typical cross-section of GFRP-RC slab.

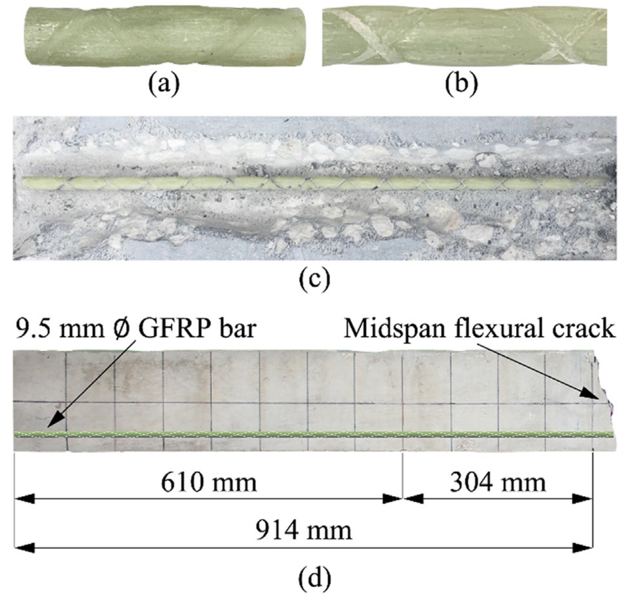

Fig. 2. Detail of surface condition and location of assessed GFRP bars: (a) pristine GFRP bar, (b) extracted GFRP bar, (c) extraction activity (bottom view), (d) side view of GFRP-RC slab and evaluated portion (610 mm).

per mix design and environmental conditioning were tested. These tests include compressive strength, bulk resistivity, surface resistivity, and ultrasonic pulse velocity (UPV) according to ASTM C39 [32], AASHTO TP 119 [33], AASHTO T 358 [34], and ASTM C597 [35], respectively. Due to different conditioning regimens, concrete samples have different moisture content; therefore, durability tests should only be compared between samples that have the same conditioning regimen. In addition, pH measurements were conducted on powdered concrete samples to obtain a quantitative estimate of its alkalinity. The test method proposed by Grubb et al. [36] was used to measure the pH of concrete due to its relative simplicity and precision [12], in which powdered concrete is diluted with deionized water (1:2) and measured with a pH meter. Powdered concrete samples were obtained by drilling at 19 mm (from the outer surface inwards), which represents the location of the GFRP bar. Table 3 summarizes the physical and mechanical properties of seawater concrete measured after 24 months of exposure.

2.2. Testing plan

To evaluate the long-term performance of GFRP bars embedded in seawater concrete, physical and mechanical properties of unconditioned pristine GFRP bars were used as the control threshold reference. The seawater-mixed GFRP-RC slabs (from where the GFRP bars were extracted) were conditioned for 1, 6, 12, and 24 months under the two environmental conditions (FC25 and SW60). Those simply supported slabs had a span between supports of 1.525 m and were tested under three-point bending load tests until failure. Considering that the GFRP-RC slabs had failed because of reinforcement rupture at midspan, the GFRP bar segments (610 mm) used to evaluate residual properties were carefully extracted from regions closer to the ends of the slabs, as shown in Fig. 2. After extraction, no visual damages were observed on the surface of the GFRP bars [Fig. 2(a) and (b)]. The mechanical properties evaluated in this study were tensile strength, longitudinal elastic modulus, transverse shear strength, and apparent horizontal shear strength, while the physical properties were glass transition temperature (T_g) and microstructural integrity through scanning electron microscopy (SEM) images and energy-dispersive X-ray spectroscopy (EDS).

2.2.1. Tensile tests

The longitudinal tensile strength and elongation properties were determined according to ASTM D7205 [37] with necessary modifications. Since GFRP-RC slabs were 1828 mm long and failed at midspan, due to GFRP bar rupture, the tensile test specimens were 914 mm long instead of the standard 980 mm as the minimum length for a 9.5-mm diameter FRP bar. The anchoring system required for testing was done by installing 300 mm long steel pipes filled with expansive mortar at both ends; therefore, the segments near the location of the GFRP bar rupture were not evaluated. Additionally, test specimens were instrumented with a 100-mm long extensometer in the middle of the free length between the anchors to capture and record tensile strain. Subsequently, the tensile test loading procedure of the extracted GFRP bars was conducted in accordance with ASTM D7205 [37]. For each period (1, 6,12, and 24 months) three (3) specimens per mix design and environmental conditions were tested. The tests were performed using a Baldwin screw gear mechanical testing machine (PC-based controller) with a capacity of 890-kN, and the load was increased at a rate of 2 mm/min until failure.

2.2.2. Transverse shear tests

The transverse shear strength tests were conducted in accordance with ASTM D7617 [38]. The principle of this test is to determine the maximum shear strength via a double shear fixture by applying a monotonic load through an upper blade until failure. Given that the GFRP bar is cut perpendicular to its longitudinal direction, the property measured in this test is directly related to the integrity of the fibers. A minimum of four (4) 225 mm long samples per mix and environmental condition, were tested for each period. The tests were performed using a 133-kN capacity

Table 3
Mechanical and durability properties of surrounding medium after 24 months of exposure.

Specimen designation	Compressive strength (MPa)	Bulk resistivity (Ω-m)	Surface resistivity (Ω-m)	UPV (m/s)	Measured pH –
F-FC25	54.1	5864	11,588	4442	11.9
F-SW60	49.9	387	887	4763	11.8
S-FC25	45.6	1550	2911	4224	11.3
S-SW60	45.0	534	1053	4568	11.5

Instron universal test frame and the load was increased in a displacement-control mode at a rate of 1.3 mm/min until failure.

2.2.3. Horizontal shear tests

The apparent horizontal shear strength test, even though its results cannot be used for design purposes, can be utilized for the comparative purpose of interlaminar-shear strength between the reference control value and the different environmental conditions. As opposed to the transverse shear strength test, this test is more related to the resin properties and controlled mostly by the fiber/resin interface integrity. The tests were performed according to ASTM D4475 [39]. A span of five times the bar diameter (47.8 mm) was used to achieve a shear mode of failure. According to the standard, GFRP bars samples shall be one diameter greater than the test span, as a result, test samples used were 58 mm long. Similar to the transverse shear test, for each exposure duration, a minimum of four (4) samples per mix and conditioning were tested. In the same way, tests were carried out in a 133-kN capacity Instron test frame using a displacement-control mode at a rate of 1.3 mm/min.

2.2.4. Glass transition temperature

The glass transition temperature, T_g, of GFRP bars were assessed by a dynamic mechanical analysis (DMA) in accordance with ASTM E1640 [40]. This test measures the viscoelastic properties, using dynamic oscillatory assessments, as a function of temperature and frequency. For the 12- and 24-month periods, three (3) T_g specimens were tested for each mix design and environmental exposure. The specimens of 1 mm × 5 mm × 50 mm were cut from the core of each GFRP bar using a water-cooled precision saw (IsoMet 1000) with a diamond blade (IsoMet 15LC). The DMA tests were conducted using a TA Instruments Dynamic Mechanical Analyzer Q800 with a three-point bending test setup. The testing parameter consisted of temperature ranging 30 to 200 °C at a heating rate of 1 °C/min and a frequency of 1 Hz.

2.2.5. Microstructural analysis

SEM observations and EDS analysis were used to evaluate the microstructure integrity of GFRP bars after environmental exposure when compared to unconditioned specimens. Samples 12.7-mm long were cut from the extracted GFRP bar segments after being exposed for 24 months. Sample preparation for SEM/EDS analysis requires a highly polished surface to obtain optimal images. Prior to imaging, GFRP bar samples were ground and polished, using a semiautomatic grinding/polishing machine (LaboForce 100) along with several levels of abrasiveness, ranging from 500 grit size to 0.04 μm polishing cloth and various water-based diamond suspension (MD-System by Struers).

SEM images were captured using a Zeiss EVO 60 SEM at the accelerating voltage of 20 kV. Since GFRP bars are a non-conductive material and the samples were not sputter-coated with a conducting metal, the variable pressure (VP) mode was used along with the backscattered electron (BSE) signal. Images were taken mainly close to the edge of the bar since fibers are more likely to be most affected by the surrounding medium. Lastly, specimens used in SEM observations were also utilized in the EDS analysis, where the main objective was to detect any change in the fiber's chemical composition. However, the EDS analysis also helped to identify the main elemental compositions, thus corroborating the type of glass fibers used to manufacture the GFRP bars.

3. Tests results and discussion

The average measured residual mechanical properties (i.e., tensile strength, tensile modulus of elasticity [Young's modulus], transverse shear strength, and apparent horizontal shear strength) of all extracted GFRP bars after environmental conditioning are summarized in Table 4. Overall, for each group of specimens, test results show a small discrepancy relative to the number of tested samples. The computed percent coefficient of variation for all experimental residual properties ranges between 1.0 and 6.7%. In addition, statistically significant differences between exposure time and environmental conditioning for residual strength were determined by two-way analysis of variance (ANOVA). The statistical differences were expressed in terms of the ratio between-group variation to within-group variation (*F*-ratio) and the probability that a result had occurred by change (*p-value*). A p-value < 0.05 was considered statistically significant, as typically adopted in statistics [41]. Typical failure modes observed in the tested concrete-embedded GFRP bars are shown in Fig. 3.

3.1. Tensile strength retention

The tensile test of GFRP bars embedded in seawater concrete showed a linear elastic behavior up to failure regardless of the environmental conditions or exposure period. Failures were usually accompanied by delamination and rupture of individual fibers just before sudden catastrophic failure. Fig. 4 shows the tensile strength retention as a function of environmental exposure and duration of immersion of embedded GFRP bars when compared to unconditioned reference (REF) values. For both mix designs, there was a statistically significant interaction between the effects of environmental conditioning and exposure time on the residual tensile strength retention, $F(4) = 10.628$, $p < 0.001$ for mix Type-F and $F(4) = 8.622$, $p < 0.001$ for mix Type-S.

The residual tensile strengths for F-FC25 specimens were 99.9, 96.7, 100.5, and 98.6% after 1, 6, 12, and, 24 months of exposure, respectively. These results indicate that after 24 months of exposure no evident losses of tensile strength were identified. It is worth noting that standard deviation error bars largely overlap, which can be interpreted that the difference is probably not statistically significant.

For the specimens in seawater at 60 °C, F-SW60, the residual tensile strength gradually decreased over time with most of the reduction occurring during the first 12 months and almost no further strength reduction in the last period. After 1, 6, 12, and 24 months of exposure, the recorded strength retentions were 93.0, 82.6, 74.9, and 73.8%, respectively. These values are considerably lower than the specimens exposed to typical field conditions (F-FC25). This suggests, to some extent, that immersing the specimens in seawater and increasing the temperature to 60 °C has a considerable effect on the tensile strength.

As shown in Fig. 4, for the S-FC25 specimens, just after 1 month an evident decrease in the residual tensile strength of 85.4% was recorded. For the 6, 12, and 24 months of exposure, the strength retentions were 88.9, 88.7, and 81.5%, respectively. Although the 1-month period value seems to be lower than that of the subsequent period (about 3.5%), when considering its variability (error bars), the trend appears to be reasonable. However, these values are notably lower than the F-FC25 specimens (made with mix Type-F), which were exposed to the same environmental conditioning during the same time. This difference in strength retention suggests that the type of concrete surrounding the GFRP bar will have a particular effect on the degradation mechanisms. Quality tests on concrete (Table 3) indicate that mix Type-F has better durability performance than mix Type-S; however, since the concrete constituents were dosed at a concrete batching plant and delivered using a ready-mix truck, caution should be exercised when interpreting the results due to the greater potential for variability as opposed to a controlled laboratory environment. Still, comparable pH measurements were obtained at 19 mm depth.

Table 4
Experimental residual mechanical properties of extracted GFRP bars.

Exposure period	Specimen designation	Tensile strength		Tensile modulus		Transverse shear		Horizontal shear	
		(MPa)	CV (%)	(GPa)	CV (%)	(MPa)	CV (%)	(MPa)	CV (%)
1 month	F-FC25	821.1	6.6	58.3	1.2	180.1	5.8	44.0	3.3
	F-SW60	764.4	1.2	56.4	1.9	188.7	4.5	43.9	6.7
	S-FC25	702.6	3.9	54.8	1.3	187.0	2.1	47.7	5.6
	S-SW60	653.1	5.7	54.4	5.5	184.5	4.8	45.2	5.4
6 months	F-FC25	795.0	1.3	54.0	2.5	182.9	2.0	45.2	1.0
	F-SW60	679.1	3.0	54.1	5.9	187.5	3.7	43.2	5.6
	S-FC25	730.7	3.4	54.4	4.0	191.8	4.5	46.3	5.8
	S-SW60	619.8	2.1	54.5	3.4	183.0	3.1	46.7	3.3
12 months	F-FC25	826.6	3.4	53.2	2.8	189.7	6.1	43.6	5.1
	F-SW60	615.7	6.6	52.8	3.1	186.3	5.6	43.4	2.6
	S-FC25	729.1	2.5	56.1	1.7	187.2	4.8	45.5	2.1
	S-SW60	539.5	4.0	51.3	6.1	186.9	1.1	44.5	1.2
24 months	F-FC25	810.7	4.4	55.0	3.8	189.7	5.5	44.3	2.9
	F-SW60	606.9	2.3	52.3	1.2	176.6	4.6	42.5	4.2
	S-FC25	670.2	6.6	54.0	6.1	189.7	6.4	45.2	5.5
	S-SW60	568.0	5.1	55.8	5.9	177.8	5.2	43.9	2.2

Note: CV = coefficient of variation.

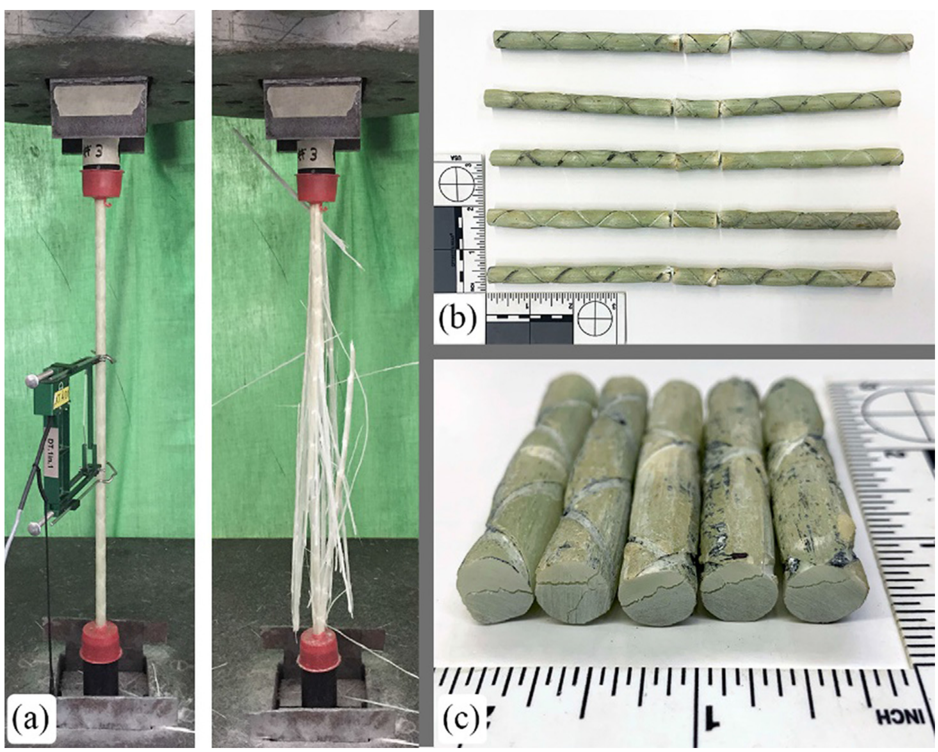

Fig. 3. Typical failure mode of extracted GFRP bars specimens after (a) tensile, (b) transverse shear, and (c) horizontal shear test.

For the S-SW60 specimens, which were the other group of concrete-embedded GFRP bars that were exposed to seawater at 60 °C, a significant reduction in the tensile strength of 79.4% (reduction by 20.6%) was recorded after the first month of exposure. Subsequently, the strength retention decreased to 75.4, 65.6, and 69.1% after 6, 12, and 24 months of exposure, respectively. The modest increase noted in the strength (about 3.5%) after the 12-month period should be interpreted with caution due to the closeness of mean values and variability.

The tensile strength reduction to a large extent may be due to a combination of various degradation mechanisms. Based on the technical literature related to FRP composites, two of the most common degradation processes are fiber integrity and degradation of fiber/resin interface [2,21,22,27]. The former is related to the resistance (at the fiber level) of the fiber itself against alkaline/chemical attack (preventing fiber dissolution), while the latter is more associated with the resin matrix softening and/or debonding at the interface. Both mechanisms affect the way the load is transferred between the fibers and the resin matrix causing a loss in the ultimate strength. These durability issues are related to each other and are known to be caused by hydrolysis reaction and moisture absorption (diffusion through the resin matrix) [2,21,22,27].

Another possible reason could be that at high longitudinal tensile load, the difference in stiffness of the constituents (fiber and resin matrix) and the presence of moisture will generate dissimilar internal strains inducing local stresses concentration at the fiber/resin interface. Ultimately, these stresses will affect mechanical interlocking which will trigger cracking and debonding between the fiber and the resin matrix causing premature failure. This can be further explained by evaluating the effect of saturation degree

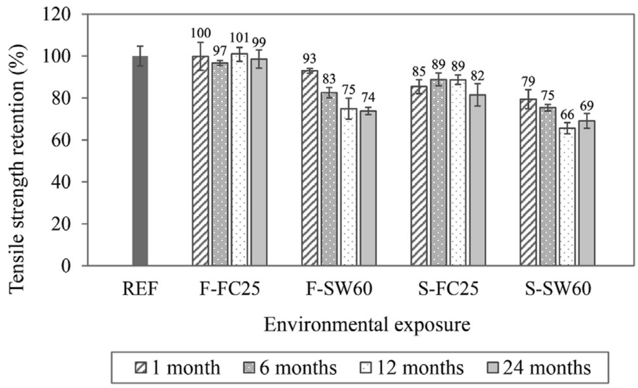

Fig. 4. Tensile strength retention of extracted GFRP bars aged in seawater concrete. Error bars represent standard deviation.

on tensile strength. Huang and Aboutaha [42], in a systematic review, discussed the effect of moisture (in the form of RH) on the degradation of embedded GFRP bars. They indicated that at 70% of ambient RH the content of capillary and absorbed water in concrete is about 21%. Therefore, regardless of whether the specimens are immersed in water or not, GFRP bars embedded in concrete can absorb moisture and water contained in capillary pores, which seep into the resin matrix thus affecting the fiber/resin interface [25,43].

3.2. Tensile modulus retention

Fig. 5 shows the retention of Young's modulus of extracted GFRP bars after 1, 6, 12, and 24 months of exposure. Evidently, from the calculated results, no obvious trend with respect to losses in elastic modulus and exposure time was identified. Similar results have been reported in the literature by different researchers [16,18–20,22–24]. Furthermore, there were no statistically significant differences detected between the effects of environmental conditioning and exposure time on the residual tensile modulus of elasticity, F = 1.720, p = 0.183 for specimens made with mix Type-F and F = 1.831, p = 1.62 for specimens made with mix Type-S.

When an analysis of the main effect of exposure time was performed, it was found that, in the case of specimens made with mix Type-F, there was a statistically significant effect $F = 5.32$, $p < 0.004$. Meaning that the duration of exposure was the parameter that most affected the residual Young's modulus rather than the conditioning environment. However, for specimens made with mix Type-S, neither exposure conditioning nor duration seems to have a major effect on the tensile modulus.

The outcomes of this research clearly reinforce the existing body of literature with respect to the degradation of strength as compared to the degradation of modulus [16,18–20,22–24]. In fact, in contrast to the strength reduction exhibited in the tensile tests, since the modulus of elasticity is obtained at a relatively low strain range (0.001-0.003) as per ASTM D7205 [37], an evident deterioration affecting load transfer between the fiber and the resin matrix may not be detected at this level of strain. Also, it has been suggested by some researchers that this phenomenon can be explained by the analytical interpretation of the composite longitudinal modulus of elasticity equation [16],

$$E_c = E_f V_f + E_m V_m \tag{1}$$

which is based on the "rule of mixtures", where E represent the modulus of elasticity, V the volume fraction, and the subscripts f and m represent fiber and matrix, respectively [6,44,45]. This equation expresses that the longitudinal Young's modulus depends on the elastic modulus and volume fraction of its constituent. The typical tensile modulus of the fiber used in this study is in the range of 80–81 GPa [46], where the resin matrix is around 4 GPa [4,6]. Considering the vast difference in magnitudes of these properties (twentyfold difference), as well as the high fiber content (71.09% by volume), the tensile modulus will mainly depend on the modulus of the fibers. Therefore, the strength reduction of elastic modulus would not be appreciated under the circumstances presented.

3.3. Transverse shear strength retention

The residual transverse shear strength of extracted GFRP bars is shown in Fig. 6. The failure mode for all tested specimens was identical, which is characterized by generating a cut perpendicular to the longitudinal axis of the GFRP bar of the same width as the upper shear plate, regardless of the environmental conditioning or the time exposed to it. The experimental results indicate no substantial strength reduction of transverse shear strength among all tested specimens. This was validated by ANOVA, which revealed no statistically significant differences between the effects of environmental conditioning and exposure time on the transverse shear residual strength, $F = 1.194$, $p = 0.339$ for specimens made with mix Type-F and $F = 0.960$, $p = 0.443$ for specimens made with mix Type-S.

The residual transverse shear strength of specimens made with mix Type-F were 93.4, 94.8, 98.4, and 98.4% for specimens exposed to typical field conditioning (F-FC25) and 97.9, 97.3, 96.6, and 91.6% for specimens immerse in seawater at 60 °C (FSW60) after

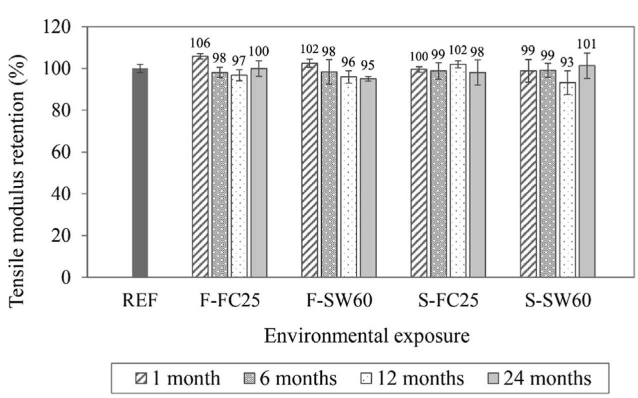

Fig. 5. Tensile modulus retention of extracted GFRP bars aged in seawater concrete. Error bars represent standard deviation.

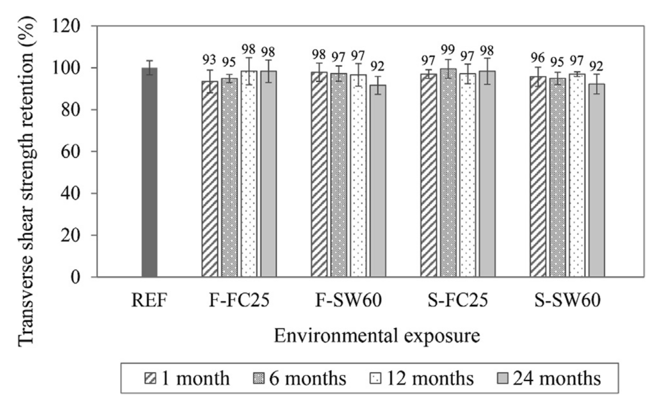

Fig. 6. Transverse shear strength retention of extracted GFRP bars aged in seawater concrete. Error bars represent standard deviation.

1, 6, 12, and 24 months of exposure, respectively. For specimens made with mix Type-S, at the end of 1, 6, 12, and 24 months of exposure, the residual transverse shear strengths were 97.0, 99.4, 97.1, and 98.4% for S-FC25 specimens and 95.7, 94.9, 96.9, and 92.2% for S-SW60 specimens. Therefore, between both mix designs, the maximum relative loss in transverse shear strength capacity after 24 months of exposure was 8%. A possible explanation for this behavior, which is the insensitivity of transverse shear to environmental conditioning, could be in the fact that fibers were not degraded by the accelerated conditioning.

3.4. Horizontal shear strength retention

The calculated apparent horizontal shear strength retention of all the tested specimens is shown in Fig. 7. All GFRP bars revealed the same failure mode characterized by a mid-depth interlaminar shear crack that developed along the length of the bar. Similar to the transverse shear strength test, no obvious degradation trend was identified. In addition, ANOVA analysis revealed no significant statistical difference between the effects of environmental conditioning and exposure time on the apparent horizontal shear residual strength, $F = 0.293$, $p = 0.880$ for specimens made with mix Type-F and $F = 0.462$, $p = 0.763$ for specimens made with mix Type-S. By running statistical analyses (ANOVA), there appears to be no significant difference; however, it seems that conditioning has some effect, because the value tends to increase when there is no conditioning and tends to decrease when there is conditioning, even though the percentage differences are very small.

The major decrease in horizontal shear strength can be attributed to the specimens conditioned in seawater at 60 °C with a maximum strength reduction of 5% and 2% after 24 months of exposure for mix Type-F and mix Type-S, respectively. These results can be compared with those reported by Gooranorimi and Nanni [12] who measured not a decrease but an increase of 4% in the horizontal shear strength on 15.9-mm diameter GFRP bars (E-glass/vinyl ester) extracted after 15 years of service. However, it should be noted that this was the product of a single test. In contrast, Manalo et al. [43] reported a horizontal shear strength reduction of 13% for 9.5-mm diameter GFRP bars (ECR-glass/vinyl ester) extracted from concrete immersed in saline solution after 112 days. Chen et al. examined the horizontal shear strength retention of 9.53-mm diameter GFRP bars (E-glass/vinyl ester) embedded in normal and high-performance concrete (HPC) and exposed to simulated HPC pore solution at 60 °C. They reported a 5 and 12% reduction in horizontal shear strength after 60 days of exposure. In fact, an even greater reduction was reported by Khatibmasjedi et al. [9] in which extracted GFRP bars decreased 26% from their original

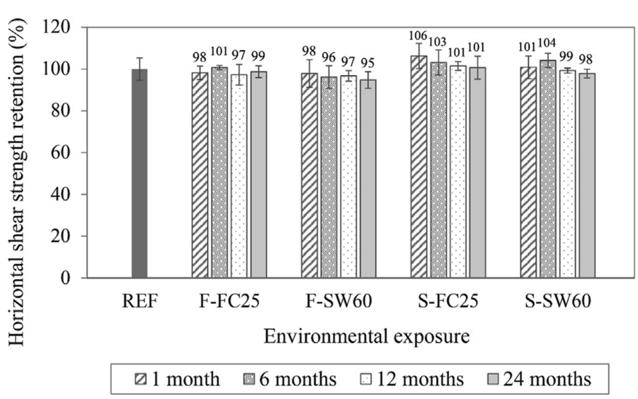

Fig. 7. Horizontal shear strength retention of extracted GFRP bars aged in seawater concrete. Error bars represent standard deviation.

horizontal shear strength after 24 months of exposure to seawater at 60 °C.

It is not well established in the literature whether the horizontal shear strength retention changes as a function of the environmental conditioning; in fact, in some cases, it decreases and in others it may even be increasing. There is no evidence that points to a specific reason and it is believed it could be several causes, including different constituent properties, surrounding medium (e.g., concrete characteristics and temperature), and manufacturing process techniques and the presence of voids/defects that are believed to ultimately increase moisture uptake, thus degrading the fiber/resin matrix interface [21,43].

3.5. Glass transition temperature

The average T_g of extracted GFRP bars after 12 and 24 months of exposure for both mix designs are summarized in Table 5. Additionally, the ratio between the conditioned specimens, $T_{g(12m)}$ and $T_{g(24m)}$ and reference values, $T_{g(ref)}$, is also provided. These values of T_g were determined by the onset of the storage modulus (E') drop. It is clear that no considerable changes in the T_g value occurred between the different conditioning environments or time of exposure. The ratio between conditioned and reference values ranged from 0.97 to 0.99. These results suggest that no significant detrimental effect on thermal properties, due to the different degree of saturation and concrete temperatures, was identified by DMA.

Even though, the moisture/humidity absorbed through the resin matrix during the aging process can decrease the T_g value [4,6], at least two possible reasons for the similarity between reference and conditioned specimens exist. First, the specimens were obtained from the center of the bar which is less prone to be affected by moisture. Second, the very small dimensions of the specimens promote the desorption of moisture during the conditioning period (40 h at 23 °C/50% RH) suggesting a reverse plasticizing effect. Furthermore, the post-curing effect of the resin matrix was also not observed, due to the fact that the temperature to which the GFRP bars were exposed was much lower than the T_g temperature (112.8 °C).

3.6. Microstructural evaluation

3.6.1. SEM images

Typical SEM cross-sectional micrographs of reference and exposed specimens that were taken near the edges of the GFRP bars are shown in Fig. 8. The main physical damages sought include fiber and/or matrix resin cracking, fiber/matrix debonding, and fiber deterioration. SEM images reveal that there were no significant differences between unconditioned (reference) and conditioned specimens after the 24-month period (beyond cracks induced during specimen preparation). Furthermore, the SEM images, irrespective of the mix designs, did not show much difference. Hence, no obvious constituent degradation of any type can be identified.

3.6.2. EDS results

The typical EDS quantitative analysis (i.e., element identification) performed on the glass fibers and the resin matrix of pristine GFRP bars are shown in Fig. 9. Results from the fiber's elemental composition revealed the main presence of silicon (Si), calcium (Ca), aluminum (Al), and oxygen (O) which is standard in commercial glass fibers. Also, traces of potassium (K), magnesium (Mg), titanium (Ti), and iron (Fe) were detected, which in turn is an indication of the type of glass, in particular, the presence of Ti as expected in ECR-glass fibers [46]. Similarly, EDS was conducted

Table 5
Results of dynamic mechanical analysis (DMA).

Specimen designation	Exposure period					
	12 months			24 months		
	Temperature (°C ± SD)	CV (%)	$\frac{T_{g(12m)}}{T_{g(ref)}}$	Temperature (°C ± SD)	CV (%)	$\frac{T_{g(24m)}}{T_{g(ref)}}$
F-FC25	110.7 ± 2.2	2.0	0.98	109.6 ± 1.6	1.5	0.97
F-SW60	109.2 ± 1.2	1.1	0.97	112.2 ± 2.1	1.9	0.99
S-FC25	112.1 ± 3.6	3.2	0.99	111.8 ± 0.1	0.1	0.99
S-SW60	112.0 ± 6.3	5.6	0.99	112.0 ± 8.4	7.5	0.99

Note: $T_{g(ref)}$ for unconditioned (as-received) value; $T_{g(12m)}$ and $T_{g(24m)}$ for values after 12 and 24 months of exposure, respectively.

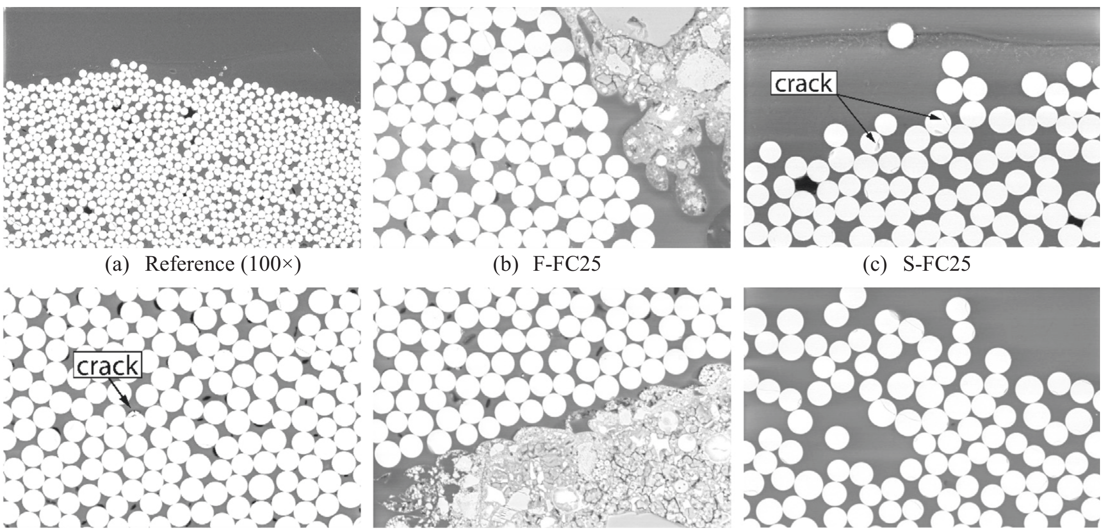

(a) Reference (100×) (b) F-FC25 (c) S-FC25
(d) Reference (300×) (e) F-SW60 (f) S-SW60

Fig. 8. Typical SEM images of unconditioned (reference) and conditioned GFRP bars cross-sections after 24 months of exposure.

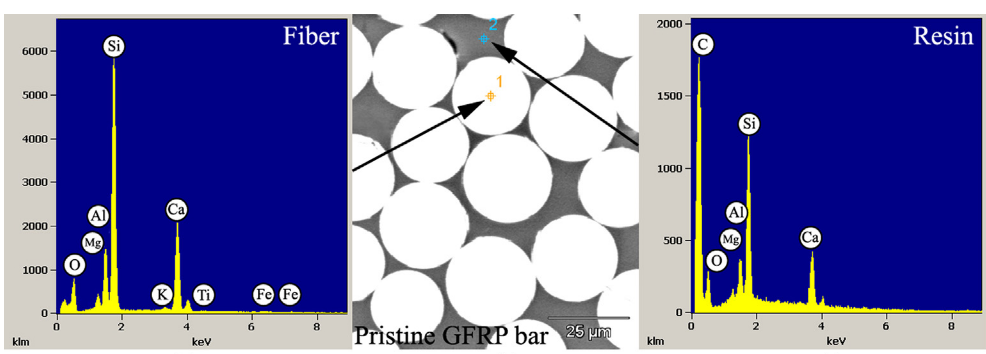

(a) (b) (c)

Fig. 9. Typical EDS spectrum of pristine GFRP bars: (a) fiberglass, (b) SEM/EDS image, (c) resin matrix.

on the resin matrix whose results indicated the characteristic peak of carbon (C) (as it should for a vinyl ester resin), in addition to minor concentrations of Si, O, Ca, and Al and traces of Mg. These small concentrations can be attributed to the use of additives and/or fillers such as aluminum silicate, calcium carbonate, and alumina trihydrate (which also acts as a flame-retardant) [4,47].

EDS quantitative analyses were performed on unconditioned and conditioned samples (24-month period) to detect potential chemical composition changes in the glass fibers, as shown in Table 6. The quantitative results revealed irrelevant differences among the main elements between the pristine and the extracted GFRP bars. Among the traced elements, perhaps the most noticeable discrepancy was found in Fe concentrations, but these values are within the margin of error for spectral resolution of EDS analysis. As a result, no apparent chemical degradation was detected in the fibers through this type of elemental microanalysis.

3.7. Prediction of long-term behavior

3.7.1. Degradation rate

Hamilton et al. [2] stated that even though internal FRP reinforcement has proven to be a suitable alternative to corrosion-prone materials, the fundamental challenge lies in the limited long-term durability data to support wider acceptance, especially in severe environmental conditions. Moreover, the American Concrete Institute in its 440.1R-15 guide acknowledged the suscepti-

Table 6
Chemical composition of glass fibers by EDS (weight percentage).

Specimen designation	Si	Ca	Al	O	Mg	K	Ti	Fe
Reference	32.52	20.80	7.16	36.86	1.68	0.46	0.32	0.22
F-FC25	32.57	21.85	7.23	35.82	1.56	0.57	0.20	0.20
F-SW60	32.50	21.41	7.26	36.02	1.62	0.62	0.32	0.25
S-FC25	32.61	21.78	7.02	36.13	1.54	0.44	0.29	0.19
S-SW60	32.38	21.55	6.94	36.58	1.59	0.52	0.28	0.16

bility of FRP bars to different environmental exposures [5]. For that reason, in this study, efforts were made to predict the long-term durability performance of the GFRP bars embedded in seawater concrete. Among the four evaluated mechanical properties (tensile strength, elastic modulus, and transverse and horizontal shear strength), the tensile strength results were the only ones that showed statistically significant differences. Hence, only the tensile strength retention values were considered to predict the long-term behavior of the GFRP bars.

Numerous researchers have evaluated different degradation models to predict the long-term mechanical properties of FRP bars. Among the most commonly used degradation rate expressions are the single and double logarithmic model, the exponential model, and the moisture diffusion model [16,48,49]. While the two logarithmic models mentioned are not associated with any specific degradation mechanism, the exponential model is assumed to model debonding at the fiber/resin interface [16] and the most frequently used moisture diffusion model is based on the one-dimensional Fickian model [50]. In this study, the exponential model was chosen to predict long-term strength retention due to the fact that, based on previous durability studies, it is the model that best fits the experimental data [16,19,49].

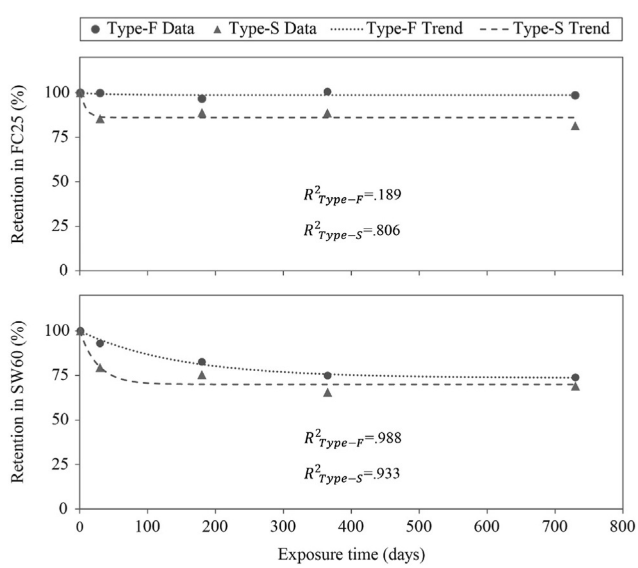

Fig. 10. Exponential degradation model fitted to the tensile strength retention values.

The following exponential degradation model was fitted to the experimental data to assess its suitability based on the coefficient of determination (R^2),

$$Y = (100 - Y_\infty)\exp(t/\tau) + Y_\infty \quad (2)$$

where Y_∞ is the retention at time infinity, t represents the exposure time, and τ is the exponential constant. The tensile strength retention values (Fig. 4) were used in Eq. (2) to obtain the exponential constant, τ, by regression analysis. A R^2 value of 0.80 is considered the minimum value for acceptability [24]; lower values indicate a lack of correlation between the experimental data points and the mathematical expression. As shown in Fig. 10, the exponential model showed an appropriate fit with R^2 values above 0.80 except for F-FC25, as expected since no degradation was observed in this particular environmental conditioning.

Based on the exponential model, a rapid degradation occurs at the beginning of the service life of the GFRP bar, which will eventually converge to the long-term retention, Y_∞, as shown in Eq. (2). The long-term retention values and the time to reach that convergence for both types of concrete mix designs and environmental exposure are summarized in Table 7. As previously mentioned, it is evident that the surrounding medium (e.g. concrete) has an effect on strength retention (easily noticeable in FC25 conditioning).

3.7.2. Service life prediction

The service life predictions, specific for the environmental conditioning used in this study and applying the exponential degradation model, are shown in Fig. 11. Based on this model, specimens embedded in seawater concrete and subjected to typical field exposure of a subtropical region (FC25) would retain a tensile strength of more than 86% over the service life of the structure. Comparatively, if concrete specimens are immersed in seawater at 60 °C, strength retention of 70% or above was predicted. Overall, convergence times were reached within the first 5 years of projected trends. This is somewhat expected since, in all tested GFRP bars, the reduction in tensile strength between the last exposure periods did not decrease any further, thus this is reflected in the early convergence to the long-term strength retention (Y_∞).

Given the reason that long-term exposure of GFRP bars to different types of environmental conditions can affect tensile strength, the ACI 440 Committee established a design philosophy

Table 7
Long-term retention values.

Mix design	Environmental Exposure			
	FC25		SW60	
	Y_∞	t(years)	Y_∞	t(years)
Type-F	98.7	1.01	73.5	4.71
Type-S	86.0	0.56	70.0	0.52
Range	86.0–98.7	0.56–1.01	70.0–73.5	0.52–4.71
Average	92.4	0.80	71.8	2.6

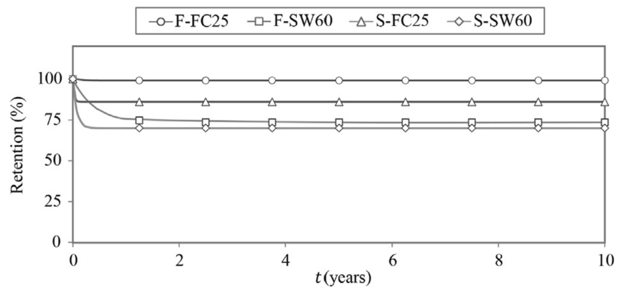

Fig. 11. Service life predictions (based on the exponential degradation model).

where the guaranteed tensile strength is altered by a safety factor known as the *environmental reduction factor* (C_E). This factor was determined based on the consensus of the ACI 440 Committee and varies between 0.70 and 1.0 (reduction of 30% to none), depending on the fiber type and exposure conditioning; 0.70 for concrete structures exposed to earth and weather and 1.0 for no such exposure. Based on the results obtained from the long-term predictions, the minimum strength retention for specimens not exposed to weathering conditioning (FC25) was 86%, thus the currently accepted C_E seems to be conservative. While for specimens exposed to seawater at 60 °C (SW60) the minimum strength retention was 70%. However, it should be noted that consistent and continuous temperatures of 60 °C are highly unlikely since the highest recorded punctual sea surface registered temperatures worldwide are around 35 °C [51]. At the same time, further validation of these outcomes and calibration of the degradation model should be compared to data obtained from existing structures that have been in service for a prolonged period of time.

4. Summary and conclusions

In this research study, the durability of unstressed GFRP bars that were embedded in seawater concrete and exposed to a typical subtropical field environment (25 °C/71.2% RH) and seawater at 60 °C were evaluated. The comparison between unconditioned and conditioned of physico-mechanical properties was an indicator of degradation. The mechanical test results include tensile strength, longitudinal elastic modulus, transverse shear strength, and apparent horizontal shear strength, while the physical evaluation comprises of T_g test results and microstructural analysis through SEM images and EDS. In addition, the exponential prediction model was used to evaluate the degradation rate of GFRP bars under different environmental conditions. In accordance with the results obtained, the following observations are made.

- The type of surrounding concrete as well as immersing the specimens in seawater and increasing the temperature to 60 °C has an effect on tensile strength retention.
- Tensile strength results showed statistically significant differences. This may be due to the presence of moisture that at high loads induces local stresses concentration at the fiber/resin interface, which in turn prompts cracks and debonding between the fiber and the resin matrix leading to premature failure.
- In contrast to the loss in tensile strength, the elastic modulus was not affected. This is mainly because the modulus of elasticity is largely governed by the glass fiber and its degradation may not be sufficiently significant to be quantified.
- Even after 24 months of exposure, transverse and shear strength results show minimal strength reduction. For example, the transverse shear strength results decreased by 2–8%, while the horizontal shear strength reduced by 1–5% of the original strength.
- No considerable microstructural changes were detected through SEM images and quantitative EDS analysis within the cross-sectional area of conditioned GFRP bars after 24 months of exposure.
- To have a better understanding of the moisture-associated degradation mechanism, since moisture can wick through the interface and accumulate in the voids, the microstructural analysis should be performed not only near the edges of the bar but also in the vicinity of voids.
- The exponential degradation model showed good agreement with the experimental data obtained from the tensile tests (R^2 values above 0.80) with the exception of specimens that exhibited no significant strength reductions.
- Based on long-term prediction and under typical field conditioning at 25 °C/71%RH, the tensile strength retention varied between 86.0 and 98.7% (avg. 92%). Under more aggressive conditioning (seawater at 60 °C), retention was predicted to range from 70.0 to 73.5%. (avg. 72%).

According to the findings of this study, the long-term performance of unstressed GFRP bars embedded in seawater concrete can be used to better evaluate strength retention and design reduction factors.

CRediT authorship contribution statement

Carlos N. Morales: Conceptualization, Methodology, Validation, Formal analysis, Investigation, Writing - original draft, Visualization. **Guillermo Claure:** Conceptualization, Methodology, Writing - review & editing, Supervision. **Alvaro Ruiz Emparanza:** Formal analysis, Investigation, Writing - review & editing. **Antonio Nanni:** Writing - review & editing, Supervision, Funding acquisition.

Declaration of Competing Interest

The authors declare that they have no known competing financial interests or personal relationships that could have appeared to influence the work reported in this paper.

Acknowledgements

The authors gratefully acknowledge the financial support from the Qatar National Research Fund by the grant # NPRP9-110-2-052 and the National Science Foundation (NSF) and its Industry/University Center for the Integration of Composites into Infrastructure (CICI) at the University of Miami under the grant # NSF-1916342. The contents stated herein are solely the responsibility of the authors.

References

[1] Bentur A, Berke N, Sidney D. Steel Corrosion in Concrete: Fundamentals and Civil Engineering Practice. London: CRC Press; 1997. https://doi.org/10.1201/9781482271898.
[2] H.R. Hamilton, B. Benmokrane, C.W. Dolan, M.M. Sprinkel, Polymer Materials to Enhance Performance of Concrete in Civil Infrastructure, Polym. Rev. 49 (1) (2009) 1–24, https://doi.org/10.1080/15583720802656153.
[3] Nanni A, De Luca A, Jawaheri Zadeh H. Reinforced Concrete with FRP Bars: Mechanics and Design. Boca Raton, Florida: CRC Press/Taylor & Francis Group; 2014. https://doi.org/10.1201/b16669.
[4] Bai J. Advanced Fibre-Reinforced Polymer (FRP) Composites for Structural Applications. Sawston, Cambridge: Woodhead Publishing Limited; 2013. https://doi.org/10.1533/9780857098641.
[5] American Concrete Institute (ACI) Committee 440. Guide for the Design and Construction of Structural Concrete Reinforced with Fiber-Reinforced Polymer (FRP) Bars. 2015.
[6] Zoghi M. The International Handbook of FRP Composites in Civil Engineering. Boca Raton, Florida: CRC Press; 2013. https://doi.org/10.1201/b15806

[7] Emparanza AR, Kampmann R, De Caso y Basalo F. State-of-the-practice of global manufacturing of FRP rebar and specifications. Am Concr Institute, ACI Spec Publ 2017;2017-Octob:717–30.
[8] Younis A, Ebead U, Suraneni P, Nanni A. Fresh and hardened properties of seawater-mixed concrete. Constr Build Mater 2018;190:276–86. https://doi.org/10.1016/j.conbuildmat.2018.09.126.
[9] Khatibmasjedi M, Ramanathan S, Suraneni P, Nanni A. Durability of Commercially Available GFRP Reinforcement in Seawater-Mixed Concrete under Accelerated Aging Conditions. J Compos Constr 2020;24:04020026. https://doi.org/10.1061/(ASCE)CC.1943-5614.0001035.
[10] El-Hassan H, El Maaddawy T. Microstructure Characteristics of GFRP Reinforcing Bars in Harsh Environment. Adv Mater Sci Eng 2019;2019:1–19. https://doi.org/10.1155/2019/8053843.
[11] Ceroni F, Cosenza E, Gaetano M, Pecce M. Durability issues of FRP rebars in reinforced concrete members. Cem Concr Compos 2006;28:857–68. https://doi.org/10.1016/j.cemconcomp.2006.07.004.
[12] O. Gooranorimi, A. Nanni, GFRP Reinforcement in Concrete after 15 Years of Service, J Compos Constr 21 (2017) 04017024, https://doi.org/10.1061/(ASCE)CC.1943-5614.0000806.
[13] V. Benzecry, J. Brown, A. Al-Khafaji, R. Haluza, R. Koch, M. Nagarajan, et al., Durability of GFRP Bars Extracted from Bridges with 15 to 20 Years of Service Life, Strateg Dev Counc Am Concr Inst (2019). https://www.acifoundation.org/Portals/12/Files/PDFs/GFRP-Bars-Full-Report.pdf.
[14] ASTM D7957. Standard Specification for Solid Round Glass Fiber Reinforced Polymer Bars for Concrete Reinforcement, West Conshohocken (PA): 2017.
[15] Chen Y, Davalos JF, Ray I. Durability Prediction for GFRP Reinforcing Bars Using Short-Term Data of Accelerated Aging Tests. J Compos Constr 2007;10:279–86. https://doi.org/10.1061/(ASCE)1090-0268(2006)10:4(279).
[16] Wang Z, Zhao X-L, Xian G, Wu G, Singh Raman RK, Al-Saadi S, et al. Long-term durability of basalt- and glass-fibre reinforced polymer (BFRP/GFRP) bars in seawater and sea sand concrete environment. Constr Build Mater 2017;139:467–89. https://doi.org/10.1016/j.conbuildmat.2017.02.038.
[17] Wang Z, Zhao X-L, Xian G, Wu G, Singh Raman RK, Al-Saadi S. Durability study on interlaminar shear behaviour of basalt-, glass- and carbon-fibre reinforced polymer (B/G/CFRP) bars in seawater sea sand concrete environment. Constr Build Mater 2017;156:985–1004. https://doi.org/10.1016/j.conbuildmat.2017.09.045.
[18] Al-Salloum YA, El-Gamal S, Almusallam TH, Alsayed SH, Aqel M. Effect of harsh environmental conditions on the tensile properties of GFRP bars. Compos Part B Eng 2013;45:835–44. https://doi.org/10.1016/j.compositesb.2012.05.004.
[19] Tu J, Xie H, Gao K. Prediction of the Long-Term Performance and Durability of GFRP Bars under the Combined Effect of a Sustained Load and Severe Environments. Materials (Basel) 2020;13:2341. https://doi.org/10.3390/ma13102341.
[20] Debaiky AS, Nkurunziza G, Benmokrane B, Cousin P. Residual Tensile Properties of GFRP Reinforcing Bars after Loading in Severe Environments. J Compos Constr 2006;10:370–80. https://doi.org/10.1061/(ASCE)1090-0268(2006)10:5(370).
[21] Chen Y, Davalos JF, Ray I, Kim H-Y. Accelerated aging tests for evaluations of durability performance of FRP reinforcing bars for concrete structures. Compos Struct 2007;78:101–11. https://doi.org/10.1016/j.compstruct.2005.08.015.
[22] Fergani H, Di Benedetti M, Miàs Oller C, Lynsdale C, Guadagnini M. Durability and degradation mechanisms of GFRP reinforcement subjected to severe environments and sustained stress. Constr Build Mater 2018;170:637–48. https://doi.org/10.1016/j.conbuildmat.2018.03.092.
[23] Tarek H Almusallam, Yousef A Al-Salloum, Saleh H Alsayed, Sherif El-Gamal, Mohammed Aqel, Tensile properties degradation of glass fiber-reinforced polymer bars embedded in concrete under severe laboratory and field environmental conditions, J. Compos. Mater. 47 (4) (2013) 393–407, https://doi.org/10.1177/0021998312440473.
[24] Mathieu Robert, Patrice Cousin, Brahim Benmokrane, Durability of GFRP Reinforcing Bars Embedded in Moist Concrete, J. Compos. Constr. 13 (2) (2009) 66–73, https://doi.org/10.1061/(ASCE)1090-0268(2009)13:2(66).
[25] Mathieu Robert, Brahim Benmokrane, Combined effects of saline solution and moist concrete on long-term durability of GFRP reinforcing bars, Constr. Build. Mater. 38 (2013) 274–284, https://doi.org/10.1016/j.conbuildmat.2012.08.021.
[26] Daoguang Jia, Qingyong Guo, Jize Mao, Jianfu Lv, Zailin Yang, Durability of glass fibre-reinforced polymer (GFRP) bars embedded in concrete under various environments. I: Experiments and analysis, Compos. Struct. 234 (2020) 111687, https://doi.org/10.1016/j.compstruct.2019.111687.
[27] Hilal El-Hassan, Tamer El-Maaddawy, Abdelrahman Al-Sallamin, Abdullah Al-Saidy, Performance evaluation and microstructural characterization of GFRP bars in seawater-contaminated concrete, Constr. Build. Mater. 147 (2017) 66–78, https://doi.org/10.1016/j.conbuildmat.2017.04.135.
[28] Jianzhuang Xiao, Chengbing Qiang, Antonio Nanni, Kaijian Zhang, Use of sea-sand and seawater in concrete construction: Current status and future opportunities, Constr. Build. Mater. 155 (2017) 1101–1111, https://doi.org/10.1016/j.conbuildmat.2017.08.130.
[29] Carlos N. Morales, Guillermo Claure, Jorge Álvarez, Antonio Nanni, Evaluation of fiber content in GFRP bars using digital image processing, Compos. B Eng. 200 (2020) 108307, https://doi.org/10.1016/j.compositesb:2020.108307.
[30] SEACON. Deliverable D2.4 - Sustainable concrete using seawater, salt-contaminated aggregates, and non-corrosive reinforcement. 2015.
[31] Luca Montanari, Prannoy Suraneni, Marisol Tsui-Chang, Morteza Khatibmasjedi, Usama Ebead, Jason Weiss, Antonio Nanni, Hydration, Pore Solution, and Porosity of Cementitious Pastes Made with Seawater, J. Mater. Civ. Eng. 31 (8) (2019) 04019154, https://doi.org/10.1061/(ASCE)MT.1943-5533.0002818.
[32] ASTM C39. Standard Test Method for Compressive Strength of Cylindrical Concrete Specimens, West Conshohocken (PA): ASTM International; 2017.
[33] AASHTO TP 119. Standard Method of Test for Electrical Resistivity of a Concrete Cylinder Tested in a Uniaxial Resistance Test, Washington, D.C: AASHTO; 2015.
[34] AASHTO T 358. Standard Method of Test for Surface Resistivity Indication of Concrete's Ability to Resist Chloride Ion Penetration, Washington, D.C: AASHTO; 2015.
[35] ASTM C 597. Standard Test Method for Pulse Velocity Through Concrete, West Conshohocken (PA): ASTM International; 2016.
[36] Grubb JA, Limaye HS, Kakade AM. Testing pH of concrete. Concr Int 2007;29:78–83.
[37] ASTM D7205. Standard Test Method for Tensile Properties of Fiber Reinforced Polymer Matrix Composite Bars, West Conshohocken (PA): ASTM International; 2016.
[38] ASTM D7617. Transverse Shear Strength of Fiber-reinforced Polymer Matrix Composite Bars, West Conshohocken (PA): ASTM International; 2011.
[39] ASTM D4475. Standard Test Method for Apparent Horizontal Shear Strength of Pultruded Reinforced Plastic Rods By the Short-Beam Method, West Conshohocken (PA): ASTM International; 2016.
[40] ASTM E1640. Standard Test Method for Assignment of the Glass Transition Temperature By Dynamic Mechanical Analysis, West Conshohocken (PA): 2013.
[41] Turner J, Thayer J. Introduction to Analysis of Variance: Design, Analysis & Interpretation. Thousand Oaks, CA: SAGE Publications, Inc.; 2001. https://doi.org/10.4135/9781412984621.
[42] Jianwei Huang, Riyad Aboutaha, Environmental Reduction Factors for GFRP Bars Used as Concrete Reinforcement: New Scientific Approach, J. Compos. Constr. 14 (5) (2010) 479–486, https://doi.org/10.1061/(ASCE)CC.1943-5614.0000122.
[43] Allan Manalo, Ginghis Maranan, Brahim Benmokrane, Patrice Cousin, Omar Alajarmeh, Wahid Ferdous, Ray Liang, Gangarao Hota, Comparative durability of GFRP composite reinforcing bars in concrete and in simulated concrete environments, Cem. Concr. Compos. 109 (2020) 103564, https://doi.org/10.1016/j.cemconcomp.2020.103564.
[44] Kaw AK. Mechanics of Composite Materials. 2nd ed. Boca Raton: CRC Press; 2005. https://doi.org/10.1201/9781420058291.
[45] Gibson RF. Principles of Composite Material Mechanics. 3rd ed. Boca Raton: CRC Press; 2011. https://doi.org/10.1201/b14889.
[46] Wallenberger FT, Watson JC, Li H. ASM Handbook: Composites. vol. 21. ASM International; 2001. https://doi.org/10.31399/asm.hb.v21.9781627081955.
[47] Bank LC. Composites for Construction: Structural Design with FRP Materials. Hoboken, NJ, USA: John Wiley & Sons, Inc.; 2006. https://doi.org/10.1002/9780470121429.
[48] Kampmann R, De Caso y Basalo F, Roddenberry M, Emparanza AR. Performance Evaluation of Glass Fiber Reinforced Polymer (GFRP) Reinforcing Bars Embedded in Concrete Under Aggressive Environments. Final Rep 2018:244. http://ftp.fdot.gov/file/d/FTP/FDOT LTS/CO/research/Completed_Proj/Summary_SMO/FDOT-BDV30-977-18-rpt.pdf.
[49] Julio F Davalos, Yi Chen, Indrajit Ray, Long-term durability prediction models for GFRP bars in concrete environment, J. Compos. Mater. 46 (16) (2012) 1899–1914, https://doi.org/10.1177/0021998311427777.
[50] Jun Wang, Hota GangaRao, Ruifeng Liang, Weiqing Liu, Durability and prediction models of fiber-reinforced polymer composites under various environmental conditions: A critical review, J. Reinf. Plast. Compos. 35 (3) (2016) 179–211, https://doi.org/10.1177/0731684415610920.
[51] Ocean: Sea surface temperature (1 Month - AVHRR, 1981-2006). NASA Earth Obs n.d. https://neo.sci.gsfc.nasa.gov.